

## NOTE

## A dynamic optical imaging phantom based on an array of semiconductor diodes

Jeremy C Hebden, Teresa Correia, Imran Khakoo, Adam P Gibson  
and N L Everdell

Department of Medical Physics & Bioengineering, University College London, Gower Street,  
London WC1E 6BT, UK

Received 25 July 2008, in final form 16 September 2008

Published 8 October 2008

Online at [stacks.iop.org/PMB/53/N407](http://stacks.iop.org/PMB/53/N407)

### Abstract

An electrically-activated phantom for evaluating diffuse optical imaging systems has been designed based on an array of semiconductor diodes which are used to heat a thermochromic dye embedded in a solidified polyester resin with tissue-like optical properties. The array allows individual diodes to be addressed sequentially, thus simulating the movement of a small volume of contrasting optical absorption. Two designs of diode-array phantom are described and results of imaging experiments are presented.

### 1. Introduction

Techniques for imaging biological tissues with light have been developed which exploit the significant difference between the characteristic absorptions of the oxygenated and deoxygenated forms of haemoglobin at near-infrared wavelengths to reveal localized changes in blood volume and oxygenation (Gibson *et al* 2005). Imaging generally involves placing an array of optical fibres in contact with the tissue, and measuring the light which has propagated between one fibre and another after having been scattered within the tissue beneath the array. A major application of such methods is the measurement and localization of the haemodynamic response within specific cortical regions of the brain to sensory stimuli and/or cognitive tasks. Such responses normally occur over a period of several seconds, although activity at a much faster timescale has also been observed (Gratton *et al* 2005). The increasing popularity of optical imaging systems as research tools for studying brain activity has motivated efforts to develop appropriate tissue-equivalent phantoms to evaluate such systems in the laboratory (Pogue and Patterson 2006). Of particular interest are phantoms that can mimic the spatial and temporal variability associated with optical imaging of cortical activity. While several designs of dynamic phantom have been proposed based on liquids, solid phantoms are often preferable because they do not require a containing vessel, they are more easily stored and transported, and they are usually more stable over time. A solid dynamic phantom containing a reversible, electrically-activated region has been developed by NIRx Medical Technologies

(USA). The phantom consists of an electrochromic material embedded in a solid plastic, whose optical opacity can be modulated with millisecond response times (Barbour *et al* 2006). More recently, we proposed an alternative design of electrically-activated solid phantom, based on thermochromic pigment which changes colour in response to a change in temperature (Hebden *et al* 2008). The development of a battery-operated prototype phantom containing two thermochromic targets was described, and its optical and temporal characteristics were assessed.

In this note we describe and demonstrate an efficient method of sequentially activating an arbitrary number of different thermochromic regions within a phantom, effectively representing the movement of a small volume of contrasting optical absorption. Two basic designs of phantom are briefly described, and images generated using a multi-channel optical topography system are presented.

## 2. Phantom design

The basic components of the electrically-activated solid phantom described earlier are a polyester resin (Alec Tiranti Ltd, UK), titanium dioxide particles to provide tissue-like scattering and a black thermochromic pigment (ChromaZone<sup>®</sup> powder, Thermographic Measurements Co. Ltd, UK). On heating, the pigment changes from black to white over a temperature range of about 5 °C, centred at about 47 °C. The phantom consisted of a resin block in which two cylindrical targets were embedded. The targets were impregnated with different concentrations of thermochromic pigment, and each contained a small heating resistor and a pre-calibrated thermistor. In the new design, the resistors are replaced with a network of semiconductor diodes, as illustrated in figure 1(a). Sixteen diodes are arranged as shown with the cathodes connected in four rows of four, and the anodes connected in four columns of four. Each row and column is connected to a 1 mm push-in socket embedded into the side of the resin block. Thus each diode can be 'addressed' by applying a forward bias via an appropriate pair of sockets. This heats the selected diode while all other current pathways contains at least one reverse biased diode, and no current flows through the remaining fifteen. For the diodes used (1N4937, ON Semiconductor), a forward bias voltage of 1.2 V at room temperature typically gives a forward current of about 2 A, and thus a heating power of about 2.4 W. Two designs of phantom were constructed and evaluated, based on this same diode arrangement.

### 2.1. Design 1

The first design of phantom (P1) involves distributing a known concentration of thermochromic pigment evenly throughout the entire block of resin in which the network of diodes is embedded. The concentration of pigment in resin was 0.4 mg cm<sup>-3</sup>, which earlier measurements indicate produces a decrease in absorption coefficient from 0.040 mm<sup>-1</sup> to 0.023 mm<sup>-1</sup> at a wavelength of 690 nm when heated above the activation temperature of 47 °C. The first stage of manufacture involved filling a 150 mm × 110 mm rectangular polyethylene box with a 5 mm thick layer of resin mixed with the pigment and a quantity of titanium dioxide particles to produce a transport scattering coefficient (or reduced scattering coefficient) of  $\mu'_s = 0.8 \pm 0.05$  mm<sup>-1</sup>. Once hardened, the diode network was then assembled on the layer within the box, with the two rows of sockets attached to the interior walls of the box using modelling clay. The remaining space within the box was then filled with resin containing identical concentrations of pigment and scattering particles. When the resin had hardened, the block was separated from the box and the modelling clay removed from the

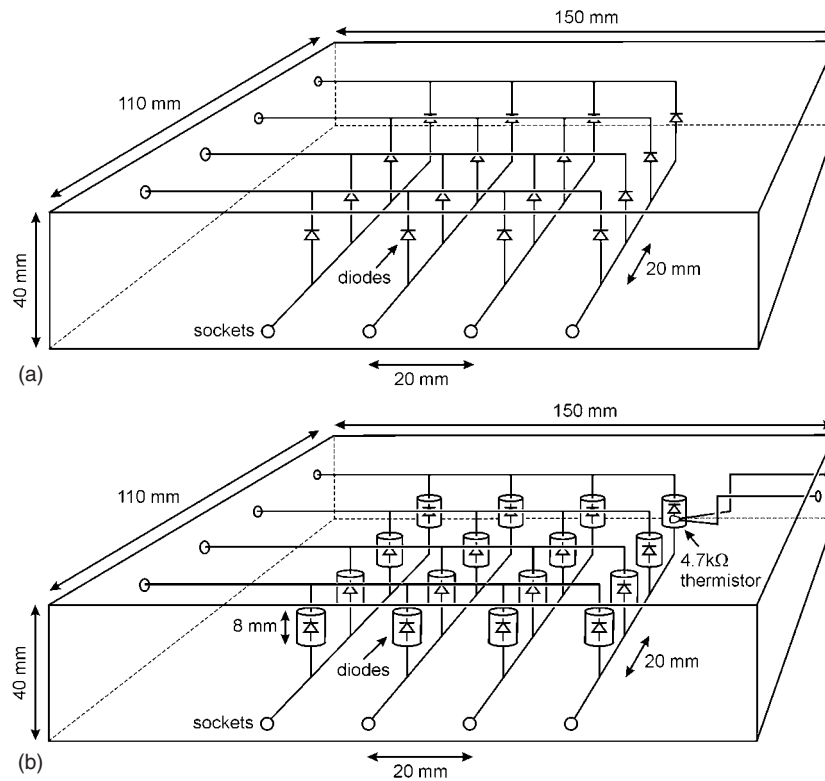


**Figure 1.** (a) First design of phantom (P1), which includes a network of 16 diodes embedded within resin containing a uniform distribution of thermochromic pigment. (b) Second design of phantom (P2), where each diode is first embedded within a cylindrical target containing thermochromic pigment. The surrounding resin does not contain the pigment. A thermistor is embedded within one target.

sockets. Finally, the block was machined to provide a flat, smooth, top surface at a height of 15 mm above the centre of each diode, as shown in figure 1(a).

Although relatively easy to construct, this design has two significant disadvantages: (i) the region over which the absorption change occurs on heating is not confined to a known volume; and (ii) increasing the magnitude of the absorption change by increasing the concentration of pigment will also increase the overall absorption of the phantom (which decreases the signal-to-noise ratio). The following design overcomes these limitations.

## 2.2. Design 2

The second design (P2) involves initially embedding each diode within a small discrete target, which contains the thermochromic pigment, while the surrounding resin is pigment free. Targets were generated by inserting each diode and the pigment-impregnated resin within a small plastic cylindrical tube. The concentration of pigment was  $16 \text{ mg cm}^{-3}$ , sufficient to produce a decrease in absorption of  $0.6 \text{ mm}^{-1}$  at a wavelength of  $690 \text{ nm}$  when heated above the activation temperature. When extracted from the tube, each target was an 8 mm diameter cylinder with a height of 8 mm, as shown in figure 1(b). For one target only, a pre-calibrated

4.7 k $\Omega$  bead thermistor was also set inside the target, to enable the heating characteristics of a diode to be evaluated. Manufacture of the second phantom block then proceeded as before, but without the pigment in the surrounding resin. The network of targets was assembled on 5 mm thick layer of resin inside an identical box, with an additional pair of sockets attached to the wall, connected to the thermistor. Again, the surrounding space was filled with resin, and the solidified block was machined to provide a smooth flat surface at a height of 15 mm above the centre of each diode. The resin block surrounding the targets was given a transport scattering coefficient  $\mu'_s = 0.8 \pm 0.05 \text{ mm}^{-1}$  and an absorption coefficient  $\mu_a = 0.001 \pm 0.0002 \text{ mm}^{-1}$  over the 650–850 nm wavelength range.

### 3. Phantom measurements

#### 3.1. Thermal characteristics

The thermal and optical properties of the thermochromic dye mixed with polyester resin were investigated in detail earlier and are described by Hebden *et al* (2008). Broadband transmittance measurements obtained across phantom P2, with the source and detector located in line with the target in which the thermistor is embedded, confirmed that a heating power of 2.75 W for 70 s is sufficient to raise the target from room temperature to a few degrees above the activation temperature and produce a significant change in transmitted intensity. Measurements also revealed that a further 25 s were required following 70 s of heating before all the thermochromic pigment within the target reverted to its deactivated state. Obviously, the electrical energy required to raise the target back above the activation temperature subsequently will depend on the period of time allowed for the heat to dissipate. For the imaging experiments involving both phantoms described below, any given diode is heated using a fixed power of 2.75 W for a period of 70 s.

#### 3.2. Optical imaging

Optical imaging of both diode-array phantoms was performed using the UCL continuous-wave optical topography system described by Everdell *et al* (2005). The measurements employed a square probe consisting of eight detectors and eight sources (operating at a single wavelength of 690 nm), identical to that employed for previous phantom (Hebden *et al* 2008) and infant brain studies (Blasi *et al* 2007). All sources are illuminated simultaneously, modulated at different frequencies. Thus each detector, sampling at 10 Hz, can isolate the diffusely reflected signal from each source by Fourier transformation.

The probe was placed on the centre of the top surface of each phantom. First, data were acquired for an initial period of 20 s, and then acquired continuously while each of the four central diodes of the array was heated in turn for 70 s, with a period of 100 s allowed for thermal dissipation between each heating period. The mean signals acquired by each source–detector combination over the initial 20 s of data were calculated and stored as a so-called reference measurement. Four further measurements were then computed by averaging signals recorded over a continuous 20 s segment of data beginning at the time the heating current for each of the four diodes was switched off. Differences between these four measurements and the reference measurement were calculated and used to reconstruct a three-dimensional (3D) image representing the change in absorption occurring within the phantom directly below the array. The linear image reconstruction algorithm solves the matrix equation  $\Delta y = J\Delta x$ , where  $\Delta y$  is the difference in signals,  $\Delta x$  is the change in absorption, and  $J$  is the Jacobian or sensitivity matrix.  $J$  is calculated using the TOAST software package (Arridge *et al* 2000) by solving

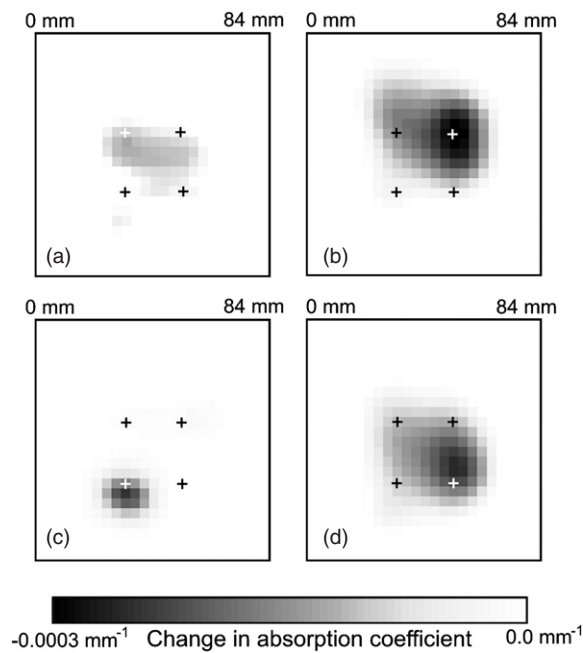


**Figure 2.** Optical topography images of phantom P1 recorded using differences in diffuse reflected intensity at 690 nm during sequential activation of the four central diodes in the following order: (a) upper left; (b) upper right; (c) lower left; and (d) lower right. The crosses represent the approximate expected positions of the diodes.

the diffusion equation for a finite element representation of the phantom/array geometry and uniform optical properties. To calculate a 3D absorption image represented by  $\Delta\mu_a$ , the matrix equation is solved using Tikhonov regularization of the Moore–Penrose generalized inverse  $\Delta\mu_a = J^T (JJ^T + \lambda I)^{-1} \Delta y$ , where  $I$  is the identity matrix and the regularization parameter  $\lambda$  was set to 0.1% of the largest singular value of  $JJ^T$ . Scattering within the phantom remains constant during heating, and thus is held at a constant value in the reconstruction.

Figure 2 shows four horizontal slices across 3D images of the phantom P1, corresponding to a depth of 15 mm below the surface. The diodes were heated in the following order: (a) upper left; (b) upper right; (c) lower left; and (d) lower right. The crosses represent the expected positions of the diodes, to within an estimated accuracy of  $\pm 3$  mm. The four images are displayed using the same greyscale. In principle, since the thermochromic pigment is distributed uniformly, contrast exhibited in these images of phantom P1 depends only on the heat distribution. While the images show isolated perturbations at locations which correlate roughly with the expected locations of the diodes, some additional features are also observed. First, we note that the initial activation (figure 2(a)) produces the lowest contrast. This is likely to be a consequence of the phantom initially being at room temperature, whereas subsequent activations produce a steady heating of the interior. Thus the heated region cools more quickly and produces lower contrast. Second, we observe that the image of the first activation exhibits a region which extends horizontally. This is probably due to heat being conducted along the wire connecting adjacent diodes which runs horizontally just below the surface of the phantom. Since the wire has a higher thermal conductivity than the surrounding resin, there is a tendency for heat to travel preferentially in this direction. For the same reason, the second activation (figure 2(b)) produces a similarly elongated feature. Meanwhile, heat will also be

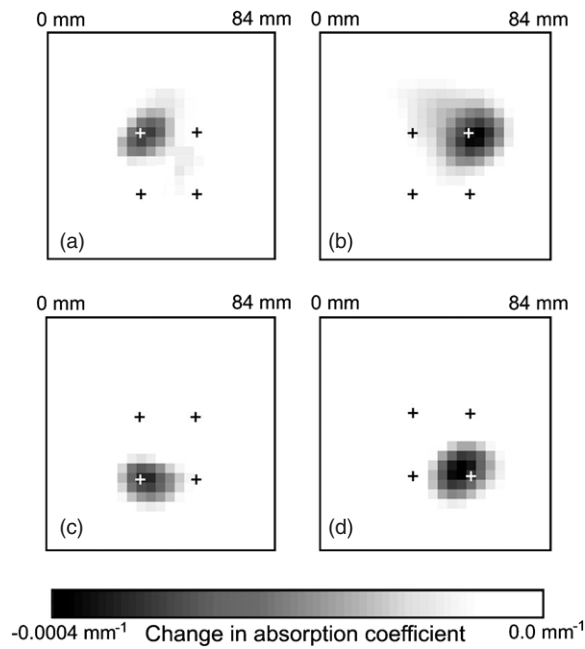


**Figure 3.** Optical topography images of phantom P2 recorded using differences in diffuse reflected intensity at 690 nm during sequential activation of the four central targets in the following order: (a) upper left; (b) upper right; (c) lower left; and (d) lower right. The crosses represent the approximate expected positions of the targets.

conducted along the wires near the lower surface of the phantom which run in the orthogonal direction. However, this is too far below the probe to be observed. The third activation (figure 2(c)) produces a more uniform perturbation, whereas the fourth (figure 2(d)) again exhibits evidence of a horizontal elongation.

It is important to note that the reconstruction method will be responsible for a degree of error in the apparent location and contrast of the perturbations. For example, there is a common tendency for isolated regions of contrast to appear closer to sources and detectors on the surface than their true locations. Earlier measurements of the properties of the thermochromic pigment at 690 nm above and below the activation temperature suggest that the maximum change in absorption for phantom P1 is about  $0.017 \text{ mm}^{-1}$ , which implies that the reconstruction has significantly underestimated the true change. However, linear image reconstruction methods are notoriously sensitive to the choice of regularization parameter  $\lambda$  as well as to the initial estimate of the optical properties used to calculate  $J$  (Gibson *et al* 2005).

Figure 3 shows four corresponding slices across 3D images of the phantom P2, also corresponding to a depth of 15 mm and displayed using a common greyscale. Diodes embedded in the discrete targets were heated in the order: (a) upper left; (b) upper right; (c) lower left; and (d) lower right. The expected positions of the diodes are again represented by crosses. All four perturbations in absorption coefficient are of similar contrast and apparent size. For this phantom, the thermochromic pigment is localized within the targets, and thus we do not expect to observe any elongation due to heating within the connecting wires. Once again, the apparent maximum change is very much less than the true decrease in absorption of the targets, estimated to be about  $0.6 \text{ mm}^{-1}$ , which underlines the poor quantitation of the reconstruction.

#### 4. Discussion

The dynamic diode-array phantoms described here are portable, very convenient to use, and are relatively easy to construct from readily available materials. The phantom which incorporates the individual targets (P2) requires somewhat more time and effort to build than the phantom with a uniform distribution of thermochromic pigment (P1), but it clearly provides more discrete and predictable regions of absorption change. Although the experiments reported above utilized a standard laboratory power supply, the phantoms can easily be battery operated. With additional thermistors and a little extra circuitry it is possible to regulate the temperature of embedded targets so that they can be maintained just above or just below the pigment activation temperature for controlled periods of time. We emphasize the value of using such a feedback control to prevent overheating, which will certainly destroy the thermochromic properties of the pigment, and could cause the phantom to disintegrate. It would also be straightforward to develop circuitry to activate diodes individually or in groups in a prescribed sequence. The limitations of these specific phantoms for evaluation of optical topography systems concern the reduced absorption change at longer near-infrared wavelengths, and the timescale of the change, which is slower than that typically associated with haemodynamic activity in the brain. However, as discussed previously (Hebden *et al* 2008), higher contrast at longer wavelengths and much faster activation times could both be achieved through appropriate selection of thermochromic pigments, the range and availability of which are likely to increase as the technology develops.

#### Acknowledgments

The work has been supported in part by the EPSRC, and by a scholarship awarded to TC by Fundação para a Ciência e a Tecnologia, Portugal.

#### References

- Arridge S R, Hebden J C, Schweiger M, Schmidt F E W, Fry M E, Hillman E M C, Dehghani H and Delpy D T 2000 A method for 3D time-resolved optical tomography *Int. J. Imaging Syst. Technol.* **11** 2–11
- Barbour R L, Graber H L, Xu Y, Pei Y, Ansari R, Levin M B and Farber M 2006 Diffuse optical tissue simulator (DOTS): an experimental calibrating system for functional DOT imaging *5th Inter-Institute Workshop on Optical Diagnostic Imaging from Bench to Bedside at the National Institutes of Health (Bethesda, MD, September 25–27, 2006)*
- Blasi A, Fox S, Everdell N, Volein A, Tucker L, Csibra G, Gibson A P, Hebden J C, Johnson M H and Elwell C E 2007 Investigation of depth dependent changes in cerebral haemodynamics during face perception in infants *Phys. Med. Biol.* **52** 6849–64
- Everdell N L, Gibson A P, Tullis I D C, Vaithianathan T, Hebden J C and Delpy D T 2005 A frequency multiplexed near-infrared topography system for imaging functional activation in the brain *Rev. Sci. Instrum.* **76** 093705
- Gibson A P, Hebden J C and Arridge S R 2005 Recent advances in diffuse optical imaging *Phys. Med. Biol.* **50** R1–43
- Gratton E, Toronov V, Wolf U, Wolf M and Webb A 2005 Measurement of brain activity by near-infrared light *J. Biomed. Opt.* **10** 011008
- Hebden J C, Brunker J, Correia T, Price B D, Gibson A P and Everdell N 2008 An electrically-activated dynamic tissue-equivalent phantom for assessment of diffuse optical imaging systems *Phys. Med. Biol.* **53** 329–37
- Pogue B W and Patterson M S 2006 Review of tissue simulating phantoms for optical spectroscopy, imaging, and dosimetry *J. Biomed. Opt.* **11** 041102